Radiation Measurements 56 (2013) 338–341

Contents lists available at SciVerse ScienceDirect

Radiation Measurements

journal homepage: www.elsevier.com/locate/radmeas

Response characterization of an Y_2O_3:Eu-based radioluminescence probe under ^{60}Co irradiation

P. Molina [a,b,*], M. Sommer [c], F. Kattner [c], J. Henniger [c]

[a] Instituto de Fisica Arroyo Seco, Universidad Nacional del Centro de la Provincia de Buenos Aires (UNICEN), Campus Universitario, Pinto 399, 7000 Tandil, Buenos Aires, Argentina

[b] Consejo Nacional de Investigaciones Científicas y Técnicas (CONICET), Rivadavia 1917, 1033 Buenos Aires, Argentina

[c] Dresden University of Technology, Institute of Nuclear and Particle Physics, Radiation Physics Group, 01069 Dresden, Germany

HIGHLIGHTS

► Y_2O_3:Eu-based fiberoptic dosimetry system.
► Red emitting phosphors makes possible use of optical filtering technique.
► Constant radioluminescence response on dose without afterglow.
► No net effect with accumulated dose in radioluminescence.

ARTICLE INFO

Article history:
Received 18 October 2012
Received in revised form
4 January 2013
Accepted 10 January 2013

Keywords:
Radioluminescence
Yttrium-oxide
Real-time dosimetry

ABSTRACT

In this work the feasibility of using Y_2O_3:Eu as a fiberoptic dosimetry (FOD) probe for real-time dosimetry has been investigated for the first time. In particular, the stability of the radioluminescence (RL) signal after repeated use and RL emission spectrum of a Y_2O_3:Eu-based fiberoptic probe have been determined. The probe has been also used to obtain a percentage depth dose curve (PDD) in a water phantom under ^{60}Co irradiation, and its performance has been compared to that of a standard ionization chamber.

1. Introduction

Real-time dose assessment dosimetry in radiotherapy with high spatial resolution is a constantly growing research field. Accurate radiotherapy techniques such as, gynaecological brachytherapy, intensity-modulated radiation therapy, intraoperative radiation therapy, stereotactic radiosurgery, among others, requires dosimeters with the characteristics mentioned before (Gagnon et al., 2012; Reniers et al., 2012; Beddar, 2007). Even though different kinds of detection systems have been investigated to perform in-vivo dosimetry, most of them lack of spatial resolution, real-time dose assessment, and intracavitary measurements. The so-called fiberoptic dosimetry (FOD) technique has shown to meet most of these requirements mostly needed in radiotherapy (Justus et al., 2004). This technique is based on the use of a tiny piece of a scintillation crystal, which is attached at the end of an optical fiber (Justus et al., 2004). The fiber collects the light emitted by the scintillator during irradiation (radioluminescence, RL) and a light detector placed at the other extreme of the optical fiber measures its intensity. In other words, FOD technique allows for in-vivo and real-time dose assessment, and since its small size not only permits accurate measurements in regions of high dose gradients but intracavitary measurements can also be performed (Spasic et al., 2011).

Stem effect is the main problem afflicting the FOD technique since this spurious luminescence produced in the optical fiber is added to the RL emission from the scintillator. Stem effect is the sum of intrinsic luminescence generated in the optical fiber by the ionizing radiation with the Cerenkov emission. The latter is usually the most relevant component of the stem effect when using PMMA optical fiber, which dominates in the blue/green spectral region (De Boer et al., 1993). Different methods have been implemented to get

* Corresponding author. Instituto de Fisica Arroyo Seco, Universidad Nacional del Centro de la Provincia de Buenos Aires (UNICEN), Campus Universitario, Pinto 399, 7000 Tandil, Buenos Aires, Argentina. Tel.: +54 249 4439660; fax: +54 223 4439669.

E-mail address: pmolina@exa.unicen.edu.ar (P. Molina).

1350-4487/$ – see front matter
http://dx.doi.org/10.1016/j.radmeas.2013.01.031

rid of Cerenkov radiation contribution. Spectral discrimination and temporal separation techniques have been successfully employed when using plastic scintillator and Al_2O_3:C-based FOD probes (Andersen et al., 2006; Clift et al., 2002; Damkjaer et al., 2008; Fontbonne et al., 2002). These techniques are needed generally when the spectrum of the RL emission partially overlaps with that of Cerenkov radiation. In spite of the success of these techniques, the simplest and cheapest technique to remove stem effect consist in using longpass optical filters (Marckmann et al., 2006) in order to reduce the spectral components of the Cerenkov emission. For this technique to be suitable, the characteristic emission of the luminescent material must be important at wavelengths higher than those where the stem effect is relevant.

Different materials have been proposed as possible FOD scintillators over the past last years (Frelin et al., 2006; Justus et al., 2004; Marcazzó et al., 2007; Molina et al., 2010, 2011a,b, 2012; Mones et al., 2006), but plastic scintillators (Archambault et al., 2006) and carbon-doped aluminum oxide (Al_2O_3:C) (Aznar et al., 2005; Damkjaer et al., 2008; Marckmann et al., 2006) have shown to be the most promising dosimeters using the FOD technique. But the intrinsic problems present in these materials, in most cases solved, encourage to search for new scintillators to be used in FOD. That is, scintillators with RL emission without dose dependence, linear response, no phosphorescence (i.e. afterglow) and emitting in the red spectral region. These desired features would make the FOD technique a simpler system, where RL signal corrections or sophisticated stem effect removing methods would not be needed.

Recent work demonstrate the feasibility of using red-emitting commercial Y_2O_3:Eu (Molina et al., 2012). Characteristics such as RL emission in the red spectral region, no changes in RL response as dose accumulates and no afterglow decay encourage further investigation. As a drawback, non-tissue equivalent responses could be expected. In this work the feasibility of using europium-doped yttrium oxide (Y_2O_3:Eu) as a FOD has been investigated for the first time. In this sense, an Y_2O_3:Eu-based FOD probe has been made and its response under ^{60}Co irradiation at a radiotherapy facility has been studied. The spectrum, stability of the RL emission, afterglow, and influence in size detector have been determined. Finally, the FOD probe has been commissioned to obtain the percentage depth dose profile (PDD) in a water phantom and the result has been compared to that obtained in identical conditions by means of a standard ionization chamber.

2. Materials and methods

Red-emitting phosphor samples, namely Y_2O_3:Eu (QK63/F-C1), kindly provided by Phosphor Technology Ltd. (UK), were used in the present work. The phosphor presents white colored powder form, with median particle grain sizes of 6 mm. The powder was glued to one of the ends of a 10 m plastic core optical fiber (PMMA, 980 microns diameter core, and 2 mm diameter outer jacket) and terminated with an SMA connector in the other end. The scintillator was optically shielded with an opaque water resistant coating in order to avoid external light. To determine the influence of the detector size, in this case corresponds to amount of powder use as scintillator, three FOD Y_2O_3:Eu-based probes were made with different amount of powder (namely Y_2O_3:Eu-1, -2, and -3).

Irradiation of the RL probes was performed in-situ (radiotherapy facility) employing a Theratron 80 ^{60}Co source, which render 0.35 Gy min^{-1} at 5 mm water depth (80 cm SSD, source to surface distance). The RL signal from the FOD probes were measured by means of a Hamamatsu H9319 photon counting photomultiplier tube (PMT) having sensitivity between 300 and 850 nm. In order to remove the stem effect contribution a longpass filter (Schott RG610), placed at the entrance of the PMT, was used.

All measurements were carried out in a water phantom (Civco MT-100) at room temperature under the reference conditions, namely, 10×10 cm^2 field and 80 cm SSD. In all cases the end of the FOD probe containing the scintillator (sensitive end) was placed at 5 mm water depth and the optical fiber was perpendicularly oriented with respect to the beam axis. The percentage depth dose (PDD) curve was determined at different depths in the water phantom by means of a manual depth dose apparatus (0.1 mm resolution). PDD profiles were determined from surface down to 150 mm. A PTW 30013 Farmer-type ionization chamber and a PTW UNIDOS E electrometer were used for reference measurements. The spectrum of the RL emission was measured by means of an Acton Research SP-2155 0.15 m monochromator with a resolution of 10 nm.

3. Results and discussion

In Fig. 1 the RL curves of the Y_2O_3:Eu-based FOD probes measured under reference conditions are shown. Difference in RL signal output is appreciated when different amount of powder is use (more than one order of magnitude between Y_2O_3:Eu-1 and Y_2O_3:Eu-3). Y_2O_3:Eu-1 refers to FOD probe with the surface of the optical fiber fully covered with Y_2O_3:Eu powder. On the other hand, Y_2O_3:Eu-3 has only a fraction of a mm diameter spot of powder centered at the surface of the optical fiber. Two important features are appreciated in this figure: stability of the RL signal output and no afterglow.

In fact, from Fig. 2 it can be appreciated that no afterglow is observable in this Y_2O_3:Eu sample and that the RL signal vanishes within a fraction of a second, almost comparable with the open/close time of the ^{60}Co drawer. According to Damkjaer et al. (2008) the negligible afterglow and the steady RL signal output could imply that no shallow traps are present in Y_2O_3:Eu scintillator. In this sense no correction for shallow traps should be made, as in Al_2O_3:C-based FOD detector.

In order to study the response stability after repeated use of the Y_2O_3:Eu probe, its RL emission has been recorded during ten consecutive irradiation cycles. The exposure time was 60 s and the lapse between irradiations 60 s. The mean value V_f of the RL intensity over exposure time for each RL curve has been computed. In principle, the value of V_f can be regarded as proportional to the dose

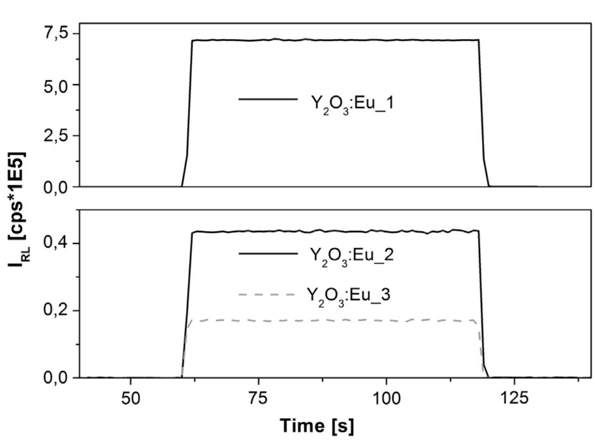

Fig. 1. RL intensity as function of time for Y_2O_3:Eu-1, Y_2O_3:Eu-2, and Y_2O_3:Eu-3 under ^{60}Co radiation. As expected, the RL signal output is proportional to amount of powder use as scintillator. The probes were irradiated at a dose rate of 0.35 Gy min^{-1}. Longpass filter with a 610 nm cut-on wavelength was employed to get rid of stem effect contribution.

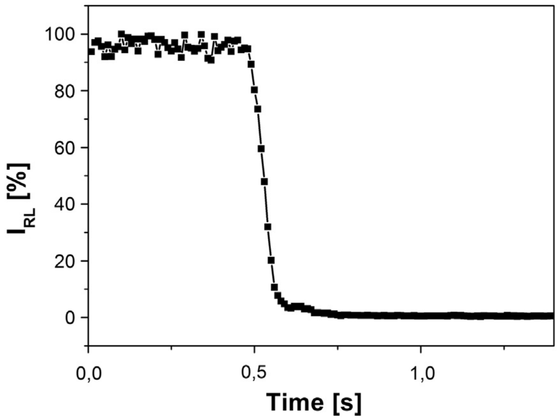

Fig. 2. Characteristic afterglow of the RL from Y_2O_3:Eu. As can be seen afterglow is negligible and RL signal vanishes within a fraction of second. 100 samples per second is the acquisition rate. The error bars corresponding to the RL measurements are comparable to the symbol size.

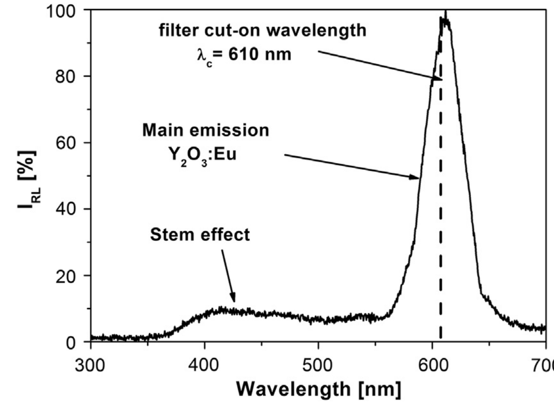

Fig. 4. RL emission spectrum from Y_2O_3:Eu without long-pass filter under ^{60}Co radiation excitation. Stem effect is the sum of Cerenkov radiation and optical fiber luminescence.

rate (Mones et al., 2006). The percentage variations of V_f, normalized by the mean values of V_f, as function of the cycle number is shown in Fig. 3. It is apparent from this figure that the RL response shows practically no significant variation over consecutive measurements. The error bars in this figure have been computed as the standard deviation of the average of the RL readings. As expected, the relative importance of the error bars increases as the RL of the different samples diminishes.

Fig. 4 shows the RL spectrum of Y_2O_3:Eu plus the stem effect from the interaction between ionizing radiation and the optical fiber. The part of the spectrum, which can be seen in this figure near 400 nm is the characteristic spectrum of the stem effect emission, which depends on the third power of the inverse of the wavelength. The strong red emission centered near 625 nm is the characteristic fluorescence of Eu^{3+}, acting as luminescence center under ionizing irradiation excitation, assigned to the $D_0 \rightarrow F_2$ transition (Molina et al., in press). From Fig. 4 is apparent that this emission from the Y_2O_3:Eu sample used in this work is located at higher wavelengths then that from the stem effect. In this case, it is expected that the light emitted by this phosphor is less affected by stem effect making possible its use as FOD scintillator. In this sense if a 610 nm longpass filter is used, then a reduction of 45% of the RL signal output from Y_2O_3:Eu-based FOD probe is expected while a significant 93% reduction of the stem effect can be achieved. Even though the 45% reduction of the RL signal seems to be a big loss, watching carefully at Fig. 1 (Y_2O_3:Eu-3), it can be appreciated that there is enough light to extract information from that RL signal.

Figs. 5 and 6 shows the percentage depth dose (PDD) from the three Y_2O_3:Eu-based FOD probes and the PDD from an ionization chamber to be use as reference measurement. From Fig. 5 the probe with the largest amount of powder (fully covers the surface of the optical fiber) presents the major deviation, instead, the other two probes showed a better agreement near the maximum but a similar deviation at higher depth. From Fig. 6 better agreement in the results is observed with all three FOD probes. These results can be explain taking into account the effective atomic number and the field sizes. One thing is for sure, secondary radiation increases at bigger irradiation field sizes. Since the effective atomic number ($Z_{eff} = 35.6$) from the Y_2O_3:Eu sample is big, it can be expected that the RL signal is sensitive to secondary radiation, where fotoelectric process dominates. Thus is easy to understand the differences observed between Figs. 5 and 6. Regarding the amount of powder used as scintillator it can be said that when using a small irradiation field (Fig. 6) there is no significant difference between FOD probes. It seems that the high Z_{eff} is responsible for the deviation observed in the PDD. On the other hand, when using a larger irradiation field

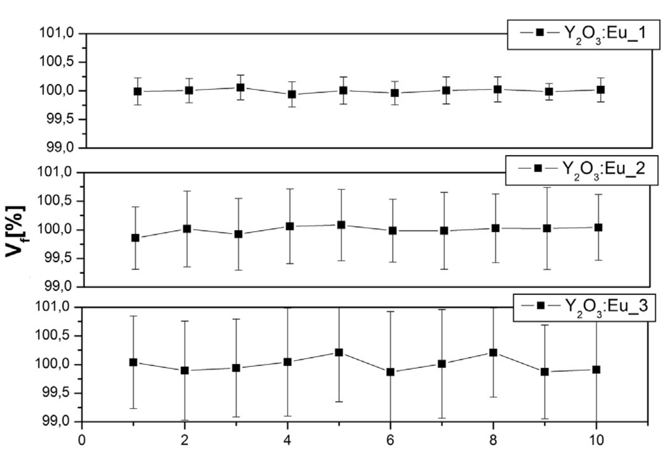

Fig. 3. RL variation of 10 consecutive measurements. Each dot represents the average of the RL signal (V_f) in the interval of irradiation time.

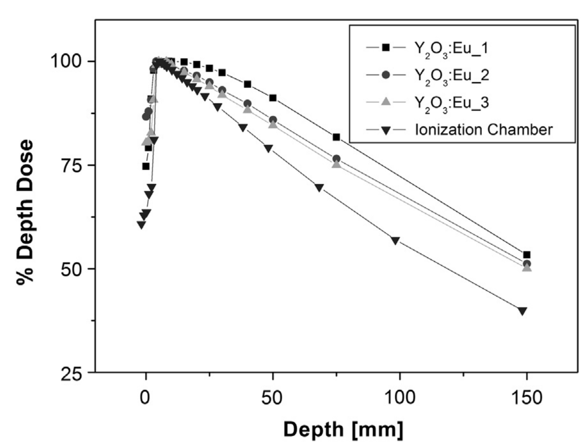

Fig. 5. PDD from Y_2O_3:Eu-based FOD compare to that of a standard ionization chamber under ^{60}Co irradiation. Surface to source distance is 80 cm and irradiation field is set to 10 × 10. The error bars corresponding to the RL measurements are comparable to the symbol size.

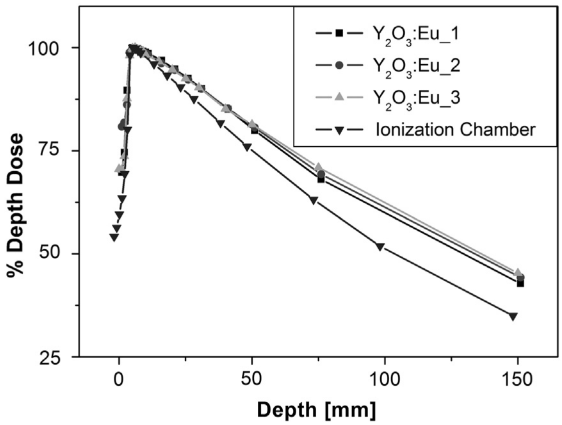

Fig. 6. PDD from Y_2O_3:Eu-based FOD compare to that of a standard ionization chamber under ^{60}Co irradiation. Surface to source distance is 80 cm and irradiation field is set to 5 × 5. The error bars corresponding to the RL measurements are comparable to the symbol size.

(Fig. 5) there is a difference in amount of powder acting as scintillator.

4. Conclusions

It has been found that Y_2O_3:Eu-based FOD probes present high sensitivity to ^{60}Co irradiation, having no changes in RL response, no afterglow and high repetitivity. The strong red emission from Y_2O_3:Eu samples allows an easy way to remove stem effect by just using a longpass filter, that is, the simplest stem effect removing technique. Regarding the differences found in PDD measurements, different coating for absorbing low energy particles from secondary radiation will be investigated in order to get a better agreement in these results. Summarizing, this work has demonstrated prospects for further research of Y_2O_3:Eu-based FOD for in vivo and real time dose assessment.

Acknowledgements

This research has been supported by Grant PICT Nr. 1907 from Agencia Nacional de Promoción Científica y Tecnológica (ANPCyT, Argentina).

References

Andersen, C.E., Marckmann, C.J., Aznar, M.C., Botter-Jensen, L., 2006. An algorithm for real-time dosimetry in intensity-modulated radiation therapy using the radioluminescence signal from Al_2O_3:C. Radiat. Prot. Dosimetry 120 (1–4), 7–13.

Archambault, L., Beddar, A., Gingras, L., 2006. Measurement accuracy and Cerenkov removal for high performance, high spatial resolution scintillation dosimetry. Med. Phys. 33, 128.

Aznar, M., Hemdal, B., Medin, J., 2005. In vivo absorbed dose measurements in mammography using a new real-time luminescence technique. Br. J. Radiol. 78, 328–334.

Beddar, A.S., 2007. Plastic scintillation dosimetry and its application to radiotherapy. Radiat. Meas. 41, S124–S133.

De Boer, S.F., Beddar, A.S., Rawlinson, J.A., 1993. Optical filtering and spectral measurements of radiation-induced light in plastic scintillation dosimetry. Phys. Med. Biol. 38, 945–958.

Clift, M.A., Johnston, P.N., Webb, D.V., 2002. A temporal method of avoiding the Cerenkov radiation generated in organic scintillator dosimeters by pulsed mega-voltage electron and photon beams. Phys. Med. Biol. 47, 1421–1433.

Damkjaer, S.M.S., Andersen, C.E., Aznar, M.C., 2008. Improved real-time dosimetry using the radioluminescence signal from Al_2O_3:C. Radiat. Meas. 43, 893–897.

Fontbonne, J.M., Iltis, G., Ban, G., Battala, A., Vernhes, J.C., Tillier, J., Bellaize, N., Le Brun, C., Tamain, B., Mercier, K., Motin, J.C., 2002. Scintillating fiber dosimeter for radiation therapy accelerator. IEEE Trans. Nucl. Sci. 49 (No 5), 2223–2227.

Frelin, A., Fontbonne, J., Ban, G., 2006. A new scintillating fiber dosimeter using a single optical fiber and a CCD camera. IEEE. Trans. Nucl. Sci. 53, 1113.

Gagnon, J.-C., Thériault, D., Guillot, M., Archambault, L., Beddar, S., Gingras, L., Beaulieu, L., 2012. Dosimetric performance and array assessment of plastic scintillation detectors for stereotactic radiosurgery quality assurance. Med. Phys. 39, 429–436.

Justus, B.L., Falkenstein, P., Huston, A.L., Plazas, M.C., Ning, H., Miller, R.W., 2004. Gated fiber-optic-coupled detector for in vivo real-time radiation dosimetry. Appl. Opt. 43, 1663–1668.

Marcazzó, J., Henniger, J., Khaidukov, N.M., Makhov, V.N., Caselli, E., Santiago, M., 2007. Efficient crystal radiation detectors based on Tb^{3+}-doped fluorides for radioluminescence dosimetry. J. Phys. D Appl. Phys. 40, 5055–5060.

Marckmann, C., Aznar, M., Andersen, C., 2006. Influence of the stem effect on radioluminescence signals from optical fibre Al_2O_3:C dosemeters. Radiat. Prot. Dosimetry 119, 363–367.

Molina, P., Prokic, M., Marcazzó, J., Santiago, M., 2010. Characterization of a fiber-optic radiotherapy dosimetry probe based on Mg_2SiO_4:Tb. Radiat. Meas. 45, 78–82.

Molina, P., Santiago, M., Marcazzó, J., Spano, F., Khaidukov, N., Caselli, E., 2011a. Radioluminescence of rare-earth doped potassium yttrium fluorides crystals. Radiat. Meas. 46, 1361–1364.

Molina, P., Marcazzó, J., Caselli, E., Khaidukov, N., Santiago, M., 2011b. $CsTb_2F_7$: an efficient radioluminescent material for fiberoptic radiation detection. Radiat. Eff. Defect. S. 166, 35–39.

Molina, P., Santiago, M., Marcazzó, J., Spano, F., Henniger, J., Craver, W., Caselli, E., 2012. Radioluminescence of red-emitting Eu-doped phosphors for fiberoptic dosimetry. Appl. Radiat. Isot. 71, 12–14.

Mones, E., Veronese, I., Moretti, F., 2006. Feasibility study for the use of Ce^{3+}-doped optical fibres in radiotherapy. Nucl. Instrum. Methods Phys. Res. A 562, 449–455.

Reniers, B., Landry, G., Eichner, R., Hallil, A., Verhaegen, F., 2012. In vivo dosimetry for gynaecological brachytherapy using a novel position sensitive radiation detector: feasibility study. Med. Phys. 39, 1925–1935.

Spasic, E., Magne, S., Aubineau-Lanièce, I., de Carlan, L., Malet, C., Ginestet, C., Ferdinand, P., 2011. Intracavitary in vivo dosimetry based on multichannel fiber-coupled radioluminescence and optically stimulated luminescence of Al_2O_3:C. In: IEEE Conference Publication. 2nd International Conference on Advancements in Nuclear Instrumentation Measurement Methods and Their Applications (ANIMMA), pp. 1–6.